HOKKAIDO UNIVERSITY

Title	Local structures of isovalent and heterovalent dilute impurities in Si crystal probed by fluorescence x-ray absorption fine structure
Author(s)	Wei, Shiqiang; Oyanagi, Hiroyuki; Kawanami, Hitoshi; Sakamoto, Kunihiro; Sakamoto, Tsunenori; Tamura, Kazuhisa; Saini, Naurang L.; Uosaki, Kohei
Citation	Journal of Applied Physics, 82(10), 4810-4815 https://doi.org/10.1063/1.366340
Issue Date	1997-11-15
Doc URL	http://hdl.handle.net/2115/50245
Rights	Copyright 1997 American Institute of Physics. This article may be downloaded for personal use only. Any other use requires prior permission of the author and the American Institute of Physics. The following article appeared in J. Appl. Phys. 82, 4810 (1997) and may be found at https://dx.doi.org/10.1063/1.366340
Type	article
File Information	JAP82-10_4810-4815.pdf

Local structures of isovalent and heterovalent dilute impurities in Si crystal probed by fluorescence x-ray absorption fine structure

Shiqiang Wei,[a] Hiroyuki Oyanagi, Hitoshi Kawanami, Kunihiro Sakamoto,
Tsunenori Sakamoto, Kazuhisa Tamura,[b] Naurang L. Saini,[c] and Kohei Uosaki[b]
Electrotechnical Laboratory, 1-1-4 Umezono, Tsukuba, Ibaraki 305, Japan

Local structures of dilute isovalent and heterovalent impurity atoms in Si crystal (Si:X, X=Ga, Ge, As) have been studied by fluorescence x-ray absorption fine structure. The distortion of local lattice around the impurity atoms was evaluated from the Si–X bond length determined by extended x-ray absorption fine structure. The results demonstrate that the local lattice deformation is strongly dependent on the electronic configuration of impurity atoms, i.e., we find an anomalous expansion $(0.09\pm0.01$ Å) along the [111] direction for donor (As) atoms but much smaller magnitude $(0.03\pm0.01$ Å) for isovalent (Ge) atoms and acceptor (Ga) atoms. The results suggest that the local lattice distortions are strongly affected by the Coulomb interactions between the localized charge, which piles up to screen the ion core and the bond charge, and the ion-core repulsion. Absence of anomaly in case of negatively charged Ga atoms suggests that the former mechanism is a dominant factor for anomalous lattice expansion. © *1997 American Institute of Physics.*
[S0021-8979(97)08822-1]

I. INTRODUCTION

The doping of crystalline Si (both thin films and bulk crystals) has numerous applications for the fabrication of advanced semiconductor devices,[1,2] which requires the state-of-the-art tailoring of a band gap (band-gap engineering). In order to understand the nature of doping-induced electronic states, it is essential to study the local structures around impurities in the doped semiconductors.

A number of articles have reported that the impurity-induced local lattice distortions modify both electronic states and crystal growth.[3–5] For example, Seki[5] found that the dislocations are reduced by Zn impurity in InP crystal. This effect has been ascribed to solution-hardening or a simple elastic interaction between impurity (solute) and dislocation.[6] The donor-complex centers formed by *n*-type doping in $GaAs_xP_{1-x}$ and (Al, Ga, In)P semiconductor alloys are well-known for doping-induced defect states.[7] In both cases, quantitative discussions require direct structural parameters around impurities. The x-ray absorption fine structure (XAFS) is a powerful technique for studying the local structure of a particular species of atom even in a complex material. XAFS has been used to obtain the structural information on the local distortion around impurities for pseudo-binary $Ga_{1-x}In_xAs$ alloys[8] and recently, dilute isovalent impurities (Ga, As) in InP.[2] For isovalent impurity atoms, the effect of alloying is often understood in terms of a virtual crystal approximation (VCA)[9] where the local distortions are treated as averaged lattice effects. However, the local atomic arrangements have been shown to deviate from the simply averaged lattice positions and the dilute impurities provide opportunities to study the lattice distortion of host atoms.[8]

It is well known that the strain caused by lattice-mismatch strongly affects the optical properties[10] and surface morphology[11] of epitaxially grown thin film semiconductors. Recently, it was revealed that the $Si_{1-x}Ge_x$ thin films on Ge(001) substrates indicate the photoluminescence spectrum due to a direct transition, where much attention has been focused on the effect of strain on the conduction band minimum. The strain also affects the surface morphology of the Si–Ge thin films. The atomic force microscopy (AFM) and transmission electron microscopy (TEM) are conventionally used to characterize the surface morphology.[12,13] However, in order to relate characteristic features of heteroepitaxial growth, such as the onset of surface roughening[11] or island formation to the mismatch strain from microscopic viewpoints, the information on the local lattice distortion is required. The elastic theories developed for predicting the band structure can be tested also if the magnitude of local distortion around dilute isovalent impurities is obtained.

Further, the information on the local distortion around heterovalent impurities would be helpful to understand the electron states of impurities from first principle calculations. In order to evaluate the effect of heterovalency as a test case, a series of heterovalent atoms in Si crystal are studied. In this article, the local structures of dilute acceptor (Ga) atoms, isoelectronic (Ge) atoms, and donor (As) atoms doped in Si crystal are reported. Fluorescence XAFS experiments have recently progressed so that impurities in the order of $10^{19}/cm^3$ can be easily studied using a multipole wiggler and a multi-element solid state detector.[14,15] On going from $Ga(s^2p^1)$ to $As(s^2p^3)$ atoms, the effect of electron configuration on the local lattice distortion can be studied since the bond lengths of impurity atoms can be obtained within ±0.01 Å precision.

II. EXPERIMENT

The Si:X (X=Ge, Ga, As) samples were prepared by either molecular beam epitaxy (MBE) or chemical vapor

---

deposition (CVD). For Si:Ge, MBE was used to grow dilute Ge–Si alloys. Details of MBE growth is descried elsewhere[16] and here the procedure is only briefly described. Boron-doped Si(001) substrate (10 Ω cm) was chemically cleaned by the Shiraki method prior to the insertion to the vacuum. The 2-μm-thick heteroepitaxial $Si_{1-x}Ge_x$ ($x = 0.006$) thin films were deposited on the substrate Si(001) surface at 673 K in a MBE growth chamber with a base pressure of 1×10^{-10} Torr.[17]

The Si:Ga sample is a Ga-doped 1.05-μm-thick Si epitaxial film with the doping concentration of 6.2 $\times 10^{18}$ cm^{-3}. The film was also grown by MBE at the substrate temperature of 900 °C on phosphorous-doped n-type Si(001) substrate with the sheet resistance of 4 Ω cm. This high dose concentration was achieved by using liquid Ga ion doping source.[18] The film was grown at the Ga ion acceleration voltage of 1 kV. The Si:As sample is an epitaxial wafer which consists of As-doped 9.6-μm-thick top layer with the doping concentration of 4.6×10^{16} cm^{-3}, and As-doped 5.4-μm-thick second layer with the doping concentration of 2.6 $\times 10^{18}$ cm^{-3}. The layers were grown on boron-doped p-type Si(111) substrate with the sheet resistance of 5 Ω cm by CVD.

The fluorescence yield spectra of Si:X (X=Ga, Ge, As) samples were measured at the BL-13B of National Laboratory for High Energy Physics (PF, KEK). The electron beam energy was 2.5 GeV and the maximum stored current was 360 mA. A 27-pole wiggler with the maximum magnetic field B_0 of 1.5 T inserted in the straight section of the storage ring was used. The calculated total power of the wiggler was 5.44 kW at $B_0 = 1.5$ T, with which the brilliance greater than by an order of magnitude from that of a bending magnet can be obtained over a wide energy range (4–30 keV). XAFS data were collected using a fixed-exit double-crystal Si(111) monochromator. The first crystal is a water-cooled flat Si(111) crystal[19] while the second crystal is a sagittally bent Si(111) crystal, which can focus the horizontal beam over ~2 mrad. A seven-element Si(Li) solid–state detector array was used to collect the fluorescence signal. The average energy resolution of each Si(Li) element with an active area of 200 mm^2 was 240 eV at 5.9 keV, using a shaping time of 6 μs. The detector output was linear below 2.5×10^4 cps after a simple correction of dead time.

For dilute Si:X samples, the large background caused by elastic scattering must be removed by an energy analysis so that a weak fluorescence yield can be measured with a high signal-to-background ratio. Figure 1 shows the energy spectrum for Si:Ga. It is clear that the elastic scattering peak is stronger than the signal Ga K_α by more than an order of magnitude. The elastic scattering peak are eliminated by using the thin Zn, Ga, and GeO$_2$ x-ray filters for the Ga, Ge, and As K-edge, respectively. With the use of an x-ray filter, the signal-to-background ratio is greatly improved as shown in Fig. 1. The energy window of the detector electronics for each channel was chosen to record only the K_α peaks of Ga, Ge, and As elements.
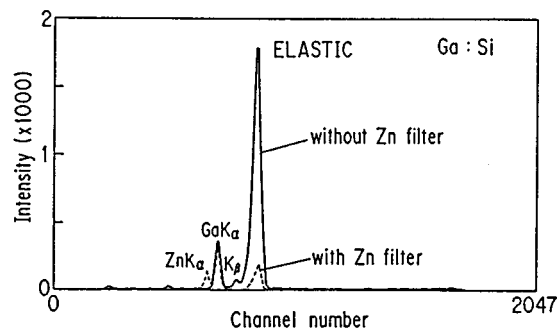

FIG. 1. Fluorescence x-ray spectrum for Si:Ga on Si(001). The elastically and inelastically scattered photons and characteristic x ray are recorded with Zn filter (dashed line) or without Zn filter (solid line).

III. RESULTS

The fluorescence yield spectra of Si:X (X=Ga, Ge, As) are shown in Fig. 2. In order to compare the EXAFS oscillations in fluorescence yield spectra, their energy positions are shifted in such a way that the position of their absorption edges coincide to zero. The absorption threshold energies are taken as 10 368 eV (Ga), 11 111 eV (Ge), and 11 868 eV (As). It can be seen that the features in the high energy region have the similar oscillations in the energy range 0–300 eV, reflecting the fact that dilute impurities substitute tetrahedral sites having a fourfold coordination with silicon atoms.

Figure 3 compares the normalized K-edge EXAFS oscillations $\chi(k)$ in the k range of 2–18 Å^{-1}. It can be readily seen that the EXAFS features are similar and the prominent oscillations appear in the low k region of 3–6 Å^{-1}. The magnitude of oscillations decreases with an increase in k showing negligible magnitude beyond 10 Å^{-1}.

The results of Fourier transform (FT) of EXAFS oscillations $k\chi(k)$ for Si:X representing the radial distribution functions (RDFs) are shown in Fig. 4. The features of the RDF are similar to those of crystalline Ge and $Si_{0.95}Ge_{0.05}$/Si(001).[20] Prominent peaks at ~2 and 3–4 Å are due to the first nearest neighbors and second and third nearest neighbors, respectively. The presence of the second and third shells indicates that impurity atoms take substitutional
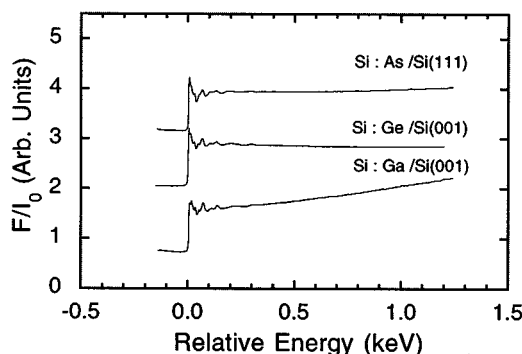

FIG. 2. Fluorescence XAFS spectra for Si:Ga, Si:Ge, and Si:As. The absorption edge energy is normalized for comparison.
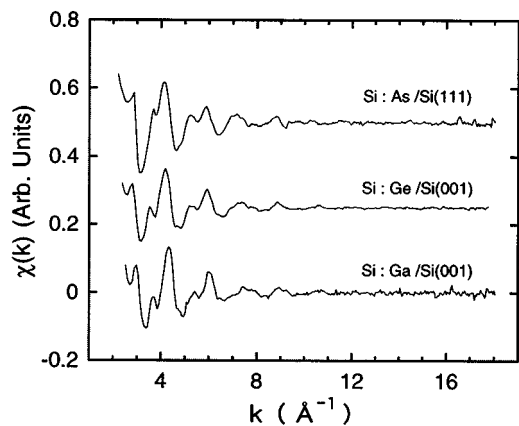
FIG. 3. EXAFS oscillations function $\chi(k)$ for Si:Ga, Si:Ge, and Si:As.

sites without degrading the medium range order. However, the tetrahedral arrangement of silicon atoms is still preserved around impurity atoms.

For getting structural parameters of nearest neighbor coordination of Ga, Ge, and As impurities, the RDFs of Si:X samples were inversely transformed to isolate the single shell EXAFS contribution. The least-squares curve fitting based on Marquart's scheme for iterative estimation of nonlinear least-squares parameters via a compromise combination of gradient, and Taylor series method[21] was used to fit the inverse transform of the EXAFS spectra. Since the concentration is low enough to neglect the impurity pairs for a random distribution, the nearest neighbor species were assumed to be silicon. Validity of such an assumption was also confirmed by the curve fit including the second shell of like-atom. The contribution of the Ga–Ga and Ga–Si pairs can be separated in a k space, because the k dependencies of the total phase-shift and backscattering-amplitude functions for Ga and Si are quite different: $|f_{Si}(k,\pi)|$ peaks at low k and falls off sharply with the increase of k while $|f_{Ga}(k,\pi)|$ has a maximum at $k=6-7$ Å^{-1} and extends to a region with $k > 15$ Å^{-1}. The theoretical amplitude function $|f_j(k,\pi)|$ and phase shift function $\Phi_{ij}(k)$ was obtained by FEFF6.[22,23] The results of curve fitting are shown in Fig. 5 and numerical results are summarized in Table I.
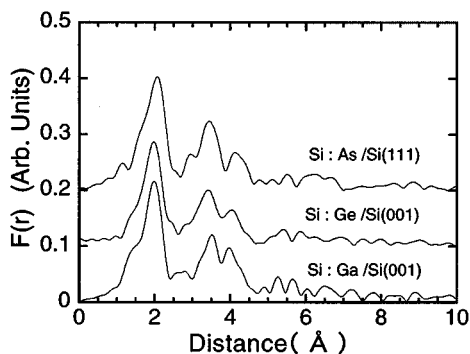

FIG. 4. Radial distribution functions obtained by FT of EXAFS oscillations for Si:Ga, Si:Ge, and Si:As.
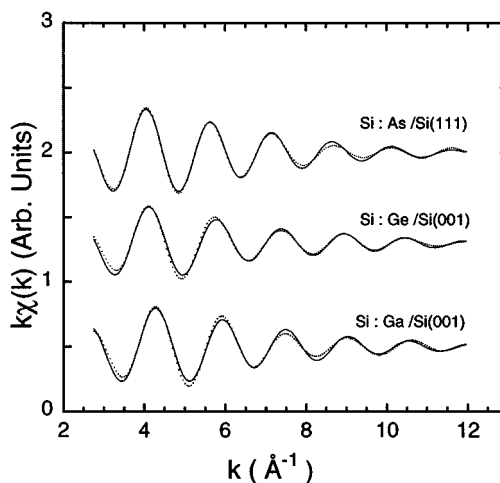

FIG. 5. Curve fit results for Si:Ga, Si:Ge, and Si:As with the single Si coordination shell model. The solid line is the experiment data and the dotted line is the fitting data.

IV. DISCUSSION

The local structures around Ga and As isoelectronic impurities doped in InP crystals have been studied by Oyanagi et al.[2] They found that the Ga–P and In–As bond lengths of impurities in InP were close to those in pure binary compounds GaP and InAs ($R_{GaP}=2.360$ Å, $R_{InAs}=2.623$ Å), deviating from the interatomic distance of InP host lattice ($R_{InP}=2.541$ Å). Such an deviation from the average lattice along the [111] direction gives rise to the local expansion or compression around impurities. Mikkelsen et al.[8] have demonstrated that, in case of pseudo-binary alloys such as $In_{1-x}Ga_xAs$, the positions of isovalent atoms (In, Ga) significantly deviate from the average lattice of a VCA crystal as theoretically predicted by Fong et al.[24] They found that the Ga–As and In–As distances take nearly constant values with a small variation of 0.04 Å. The average cation–anion distance, on the other hand, changes by 0.17 Å.

The behavior of the heterovalent impurities, i.e., whether they introduce not only a simple atomic size effect but also a new source of lattice distortion, because of a stronger interaction with host atoms is an interesting problem. Thus, it is necessary to systematically investigate the dependence of valency. Systems we studied here, Si:X (X=Ga, Ge, As) provides opportunities to study the local structure of heterovalent impurities (donor and acceptor) in comparison with the isovalent impurity. Using the XAFS technique, we have obtained the local structures for the three cases: acceptor (Ga), isoelectronic (Ge), and donor (As) impurities in Si crystal.

The RDF in Fig. 4 and XANES spectra in Fig. 6 suggest that the coordination geometry of the three cases is similar, i.e., tetrahedral coordination of Si atoms. The structural parameters (coordination number N) summarized in Table I confirm that the Ga, Ge, and As atoms are indeed coordinated by four Si atoms in the first nearest neighbor shell. Although, we have introduced the contribution of like-atom bonds (Ga–Ga, Ge–Ge, and As–As), the fit was not improved, indicating that the impurities are well-separated and the like-atom bonds can be neglected. Therefore, we con-

TABLE I. The structural parameters of Si:X crystal.

Sample	K-edge	Coordination type	R (Å)	N	σ (Å)	ΔE (eV)	ΔU_{ij} (Å)
Ga:Si(001)	Ga	Ga–Si	2.38±0.01	4.2±0.5	0.064±0.02	6.0±1.0	0.03±0.01
Ge:Si(001)	Ge	Ge–Si	2.38±0.01	3.8±0.5	0.063±0.02	4.5±1.0	0.03±0.01
As:Si(111)	As	As–Si	2.44±0.01	4.5±0.5	0.070±0.02	8.0±1.0	0.09±0.01
c-Si		Si–Si	2.35	4			

clude that the first shell of Ga, Ge, and As atoms consists of only Si atoms in agreement with an expected pair ratio ($\ll 1$) assuming a random distribution. In Fig. 6, the fact that XANES features for the three cases are similar suggests that impurity atoms have a tetrahedral coordination as in case of undistorted Si lattice.

According to Pauling's rule,[25,26] the tetrahedral covalent radii of Si, Ga, Ge, and As atoms are 1.173, 1.260, 1.225, and 1.180 Å, respectively. Their covalent bond lengths are $R_{Si-Si}=2.35$ Å, $R_{Ga-Si}=2.43$ Å, $R_{Ge-Si}=2.40$ Å, and $R_{As-Si}=2.36$ Å. The bond lengths are in the following order: $R_{Ga-Si}>R_{Ge-Si}>R_{As-Si}>R_{Si-Si}$. On the contrary, we found that the anomalous behavior as summarized in Table I. We note that the high accuracy for the bond length is achieved by systematic analysis by the curve fit using theoretical amplitude and phase shift functions. We estimate the error in bond length is ± 0.01 Å. For comparing our results with the previous studies, Fig. 7 includes the bond lengths of Si–Ga, Si–Ge, and Si–As from Phillips,[25] Oyanagi,[27] Ikeda,[28] and this work.

Although, the Si lattice is expected to expand toward the [111] direction on going from As to Ga, the results show that the R_{Ga-Si} and R_{Ge-Si} have the same value (2.38 Å) which are 0.02 Å shorter than the covalent bond lengths $R=2.40$ Å, while R_{As-Si} is 2.44 Å which is 0.04 Å longer than the sum of R_{Ge-Si} covalent radii. The local structures of the impurities are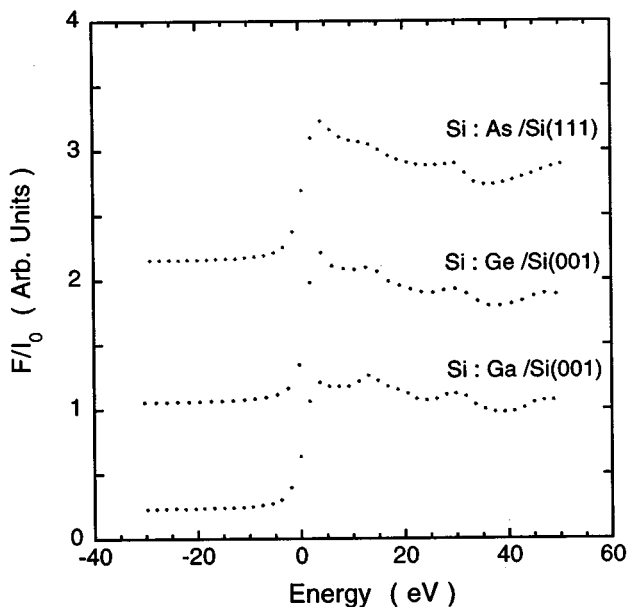 schematically illustrated in Fig. 8 where the ΔU_{ij} represents the deviation of the Si–X bond length from the Si–Si distance (2.35 Å). Erbil et al.[29] reported that the R_{As-Si} bond length is 2.41 Å for As concentrations of 0.1%–7.0%. Although our Si:As sample is more dilute and the deviation is more significant, the reported anomalously long Si–As bond is in agreement with their results. Their R_{As-Si} bond length is 0.01 Å longer than the sum of tetrahedral covalent radii of As (1.225 Å) and Si (1.173 Å)[25] and 0.03 Å shorter than our result.

However, our R_{As-Si} value is the same as the bond length of R_{As-Si} calculated by Scheffler et al. using the parameter-free self-consistent Green's function method.[30] It is a puzzling problem that the observed R_{As-Si} is 0.06 Å longer than those of R_{Ga-Si} and R_{Ge-Si}. When As atoms substitute tetrahedral sites in Si lattice with five valence electrons (s^2p^3), one surplus electron is expected to be doped while remaining four electrons are expected to form covalent bonds with Si neighbors. The fifth electron must go into the conduction band states leaving As atom to be positively charged. This extra charge of ion core is expected to rearrange the charge density around impurity atoms, i.e., the charge density increases to screen the extra charge. On the contrary, for neutral Ge atoms and negatively charged Ga atoms a charge pile up is unlikely.

It is rather surprising to find that the observed R_{As-Si} is unusually elongated while R_{Ga-Si} and R_{Ge-Si} are the same, although R_{As-Si} should be shorter than R_{Ga-Si} and R_{Ge-Si} according to the covalent radii. We note that the experimental R_{As-Si} is in agreement with the calculated value by

FIG. 6. XANES spectra for Si:Ga, Si:Ge, and Si:As. The absorption edge energy is normalized for comparison.

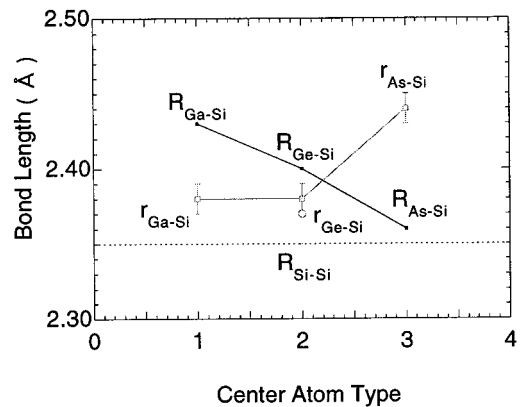FIG. 7. Bond length for Si:Ga, Si:Ge, and Si:As obtained from the previous study and this article. The $r_{Si:X}$ is taken from reference, (see Ref. 25) the open circle (r_{Si-Ge}) is taken from Oyanagi et al. (see Ref. 27), R_{Si-Si} is the bond length of crystal Si, $R_{Si:X}$ is this work.
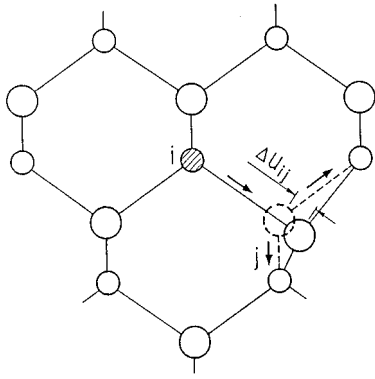
FIG. 8. Local structures for Ga, Ge, and As impurities in Si crystal. The i atom is the impurity atom, j atom is the first neighbor Si atom. ΔU_{ij} is the magnitude of the displacement of Si atom along the [111] direction.

Krüger[31] and Uhrberg[32] for symmetric As dimers absorbed on the Si(001) surface. R_{As-Si} is in the range from 2.42 to 2.44 Å, and R_{As-As} is in the range from 2.52 to 2.55 Å. In this geometry, the As atoms form s^2p^3-like bonds. Scheffler showed that the charge density at the As impurity is practically the same whether the orbital is occupied or not since As is a shallow donor in Si crystal. The unusual distortion of As–Si bond in Si crystal is interpreted in two respects. First, there is a change in the ion core at the impurity site which may increase the repulsive ion core-ion core interaction. Second, there is a pile up of charge density as a result of redistribution of bond charge in order to screen the ion core, which might increase the repulsive interaction between the charge pile up and the bond charge. Scheffler's calculations show that there are more electron density near the impurity site than is actually required for screening Si:As$^+$ in the (110) plane of the Si crystal, so that the neighbor Si valence electrons feel a repulsion and move away from the center.

For negatively charged Ga impurities, however, the observed R_{Ga-Si} is not dependent on the ion-core effect. This suggests that the electron charge density plays a dominant role in the lattice distortion. Further, the fact that the Si–X ($X=$Ga, Ge) bond length is slightly shorter than the sum of covalent radii is due to the repulsive interaction between the more extended sp^3 orbitals and those of Si atoms. For Si:Ge, the observed Si–Ge distance (2.38 Å) coincides with that for short period $(Si)_5/(Ge)_5$ superlattices[28] and the experimental value for Ge monolayer sandwiched between Si layers Si/ Ge/Si (2.37 Å) both of which are on Si(001).[27] Thus, the Ge–Si distance in strained short period Ge superlattices agrees quite well with that of Si:Ge. For strained Ge layers epitaxially grown on Si(001), a tetragonal distortion of the Ge layer is expected in order to keep the lattice spacing of the substrate constant. Since the bending force constant is smaller than that of stretching, this is achieved by the bending of both the interface Ge–Si bond and Ge–Ge bonds. This indicates that under the stress for matching the in-plane lattice spacing with that of Si lattice, the bond length relaxation at the Ge–Si interface is the same with that found for Ge impurities in Si. This means that the bond length relaxation under the lattice matching condition is essentially determined by a short range order or the first nearest neighbor coordina-

tion. This is perhaps due to the fact that bending plays an important part in distortions for lattice matching, which is determined mainly by the repulsion between the impurity atom and nearest neighbors. The observation that in Si:Ge there is only a small shift of atom positions for the second and third nearest neighbor atoms, since the distortion is mostly absorbed by the shift of neighboring atoms toward the [111] direction, which bends the second nearest bonds but hardly affects the positions of the second nearest neighbor atoms.

When the As atom replaces Si sites, its ion core is positively charged. In order to screen this charge, some electrons are transferred from the bond charge and pile up between the ion core and the bond charge. Since the interaction for both the core–core and electron–electron interactions are repulsive, nearest Si atoms are shifted away from the As impurity. As summarized in Table I, the σ disorder factors are 0.064, 0.063, and 0.070 Å for Ga–Si, Ge–Si, and As–Si covalent bonds, respectively. We note that the σ value for As:Si(111) is about 0.006 Å greater than that of both Ga:Si(001) and Ge:Si(001). This indicates that there is a larger disorder in the first shell around impurity sites in case of As:Si. Since the charge pile up to screen the ion core would weaken the bond strength, the increased relative displacement is consistent with the conclusion that the repulsion between the extra charge pile up and bond charge is a dominant factor of the local lattice distortion.

We consider that a pile up of charge density between the two ion cores is the dominating factor for repulsive interactions. The magnitude of distortion toward the [111] direction is the same for Ge and Ga. If the ion core charge plays an important role, we should observe at least the effect of the negative charge for Si:Ga. However, there is no such an effect at all. This indicates that at least the ion core charge is not the dominant factor and the repulsive force, between the pile-up electron and the bond charge is the dominating factor of local lattice distortion. The discussion is rather native but theoretical calculations would clarify the detailed mechanism of lattice expansion around impurity atoms.

V. CONCLUSION

We have determined the magnitude of the local lattice distortion around dilute impurity atoms along the [111] direction for isovalent (Ge) and heterovalent (Ga, As) atoms in Si crystal. Contrary to the systematic variation $R_{Ga-Si}>R_{Ge-Si}>R_{As-Si}$ predicted by the sum of covalent radii, we found that $R_{Ga-Si}-R_{Ge-Si}<R_{As-Si}$. The As–Si bond length is unusually long (2.44 Å) indicating that the local lattice expands by 0.09 Å. The results suggest that the local lattice distortion is not dependent on the ion-core repulsion. Instead, the present results suggest that the Si nearest neighbor atoms move away due to the repulsive interaction of a charge pile up to screen the positive charge and the bond charge. This implies that acceptor impurities introduce the local lattice expansion which should be taken into account when the energy levels of acceptor levels are discussed.

Wei *et al.*

[1] I. Shlimak, M. Kaveh, R. Ussyshkin, V. Ginodman, and L. Resnick, Phys. Rev. B **55**, 1303 (1997).

[2] H. Oyanagi, Y. Takeda, T. Matsushita, T. Ishiguro, T. Yao, and A. Sasaki, Solid State Commun. **67**, 453 (1988).

[3] A. Herrera-Gomez, P. M. Rousseau, G. Materlik, T. Kendelewicz, J. C. Woicik, P. B. Griffin, J. Plummer, and W. E. Spicer, Appl. Phys. Lett. **68**, 3090 (1996).

[4] K. C. Haas, R. J. Lempert, and H. Ehrenreich, Phys. Rev. Lett. **52**, 77 (1984).

[5] Y. Seki, J. Matsui, and H. Watanabe, J. Appl. Phys. **47**, 3374 (1976).

[6] H. Ehrenreich and J. P. Hirth, Appl. Phys. Lett. **46**, 668 (1985).

[7] J. Makinen, T. Laine, J. Partanen, K. Saarinen, P. Hautojarvi, K. Tappura, T. Hakkarainen, H. Asonen, M. Pessa, J. P. Kauppinen, K. Vanttinen, M. A. Paalanen, and J. Likonen, Phys. Rev. B **53**, 7851 (1996).

[8] J. C. Mikkelsen and J. B. Boyce, Phys. Rev. B **28**, 7130 (1983).

[9] R. Bisaro, P. Merenda, and T. P. Pearsall, Appl. Phys. Lett. **34**, 4457 (1979).

[10] T. P. Pearsall, J. Bevk, L. C. Feldman, J. M. Bonar, and J. P. Mannaerts, Phys. Rev. Lett. **58**, 729 (1987).

[11] J. E. Guyer and P. W. Voorhees, Phys. Rev. Lett. **74**, 4031 (1995).

[12] D. E. Jesson, K. M. Chen, S. J. Pennycook, T. Thundat, and R. J. Warmack, Science **268**, 1161 (1995).

[13] J. W. P. Hsu, E. A. Fitzgerald, Y. H. Xie, P. J. Silverman, and M. J. Cardillo, Appl. Phys. Lett. **61**, 1293 (1992).

[14] H. Oyanagi, R. Shioda, Y. Kuwahara, and K. Haga, J. Synchrotron Radiat. **2**, 99 (1995).

[15] L. M. Murphy, B. R. Dobson, M. Neu, C. A. Ramsdale, R. W. Strange, and S. S. Hasnain, J. Synchrotron Radiat. **2**, 64 (1995).

[16] H. Oyanagi, I. Owen, M. Grimshaw, P. Head, M. Martini, and M. Saito, Rev. Sci. Instrum. **66**, 5477 (1995).

[17] K. Sakamoto, T. Sakamoto, S. Nagao, G. Hashiguchi, K. Kuniyoshi, and Y. Bando, Jpn. J. Appl. Phys., Part 1 **26**, 666 (1987).

[18] T. Sakamoto and M. Komuro, Jpn. J. Appl. Phys., Part 2 **22**, L760 (1983).

[19] H. Oyanagi, Y. Kuwahara, and H. Yamaguchi, Rev. Sci. Instrum. **66**, 4482 (1995).

[20] H. Oyanagi, *Applications of Synchrotron Radiation to Material Analysis*, edited by H. Saisho and Y. Goshi (Elsevier, New York, 1996), p. 207.

[21] D. W. Marquart, J. Soc. Ind. Appl. Math. **11**, 431 (1963).

[22] J. J. Rehr, S. I. Zabinsky, and R. C. Albers, Phys. Rev. Lett. **69**, 3397 (1992).

[23] D. E. Sayers and B. A. Bunker, *X-ray Absorption, Principles, Applications, Techniques of EXAFS, SEXAFs, and XANES*, edited by D. C. Koningsberger and R. Prins (Wiley, New York, 1988), p. 211.

[24] C. Y. Fong, W. Weber, and J. C. Phillips, Phys. Rev. B **14**, 14 (1976).

[25] J. C. Phillips, *Bonds and Bands in Semiconductors* (Academic, New York and London, 1973), pp. 20–23.

[26] J. A. Van Vechten and J. C. Phillips, Phys. Rev. B **2**, 2160 (1970).

[27] H. Oyanagi, T. Sakamoto, K. Sakamoto, T. Matsushita, T. Yao, and T. Ishigura, J. Phys. Soc. Jpn. **57**, 2086 (1988).

[28] M. Ikeda, K. Terakura, and T. Oguchi, Phys. Rev. B **45**, 1496 (1992); *ibid.* **48**, 1571 (1993).

[29] A. Erbil, W. Weber, G. S. Gargill III, and R. F. Boehme, Phys. Rev. B **34**, 1392 (1986).

[30] M. Scheffler, Physica B & C **146**, 176 (1987).

[31] P. Krüger and J. Pollmann, Phys. Rev. B **47**, 1898 (1993).

[32] R. I. G. Uhrberg, R. D. Bringans, R. Z. Bachrach, and J. E. Northrup, J. Vac. Sci. Technol. A **4**, 1259 (1986).